Journal of Solid State Chemistry **159,** 26–31 (2001)
doi:10.1006/jssc.2001.9117, available online at http://www.idealibrary.com on IDEAL®

Gold-Coated Iron (Fe@Au) Nanoparticles: Synthesis, Characterization, and Magnetic Field-Induced Self-Assembly

Jun Lin[1]

Laboratory of Rare Earth Chemistry and Physics, Changchun Institute of Applied Chemistry, Chinese Academy of Sciences, 159 Renmin Street, Changchun 130022, People's Republic of China

and

Weilie Zhou, A. Kumbhar, J. Wiemann, Jiye Fang, E. E. Carpenter, and C. J. O'Connor

Advanced Materials Research Institute, College of Science, University of New Orleans, New Orleans, Lousiana 70148, USA

Received September 4, 2000; in revised form January 10, 2001; accepted February 9, 2001; published online May 4, 2001

A unique reverse micelle method has been developed to prepare gold-coated iron (Fe@Au) nanoparticles. XRD, UV/vis, TEM, and magnetic measurements are utilized to characterize the nanocomposites. XRD only gives FCC patterns of gold for the obtained nanoparticles. The absorption band of the Fe@Au colloid shifts to a longer wavelength and broadens relative to that of the pure gold colloid. TEM results show that the average size of Fe@Au nanoparticles is about 10 nm. These nanoparticles are self-assembled into chains on micron scale under a 0.5 T magnetic field. Magnetic measurements show that the particles are superparamagnetic with a blocking temperature (T_B) of 42 K. At 300 K (above T_B), no coercivity (Hc) and remanence (M_r) is observed in the magnetization curve, while at 2 K (below T_B) Hc and M_r are observed to be 728 Oe and 4.12 emu/g, respectively.

Key Words: **reverse micelle method; nanoparticle; iron; gold; magnetic properties; self-Assembly.**

INTRODUCTION

Due to their small size (1–100 nm), nanoparticles exhibit novel materials properties that differ considerably from those of the bulk solid state (1). Especially in recent years, the interests in nanometer-scale magnetic particles are growing based on their potential application as high-density magnetic storage media (2, 3). However, as the particle size decreases, the reactivity of the particle increases and the magnetic properties are influenced more by surface effects (4). So far the passivation of magnetic nanoparticles (γ-Fe_2O_3, Co *et al.*) by another inert layer (SiO_2, polymer *et al.*) has been developed (5–7). However, the nonmetallic layer potentially reduces the magnetic properties of the magnetic nanoparticles. We have used a sequential synthesis method to form a passivation layer of gold on metal and alloy nanoparticles (8). Gold has become a favored coating material because of a simple synthetic procedure and its chemical functionality (9). It is expected that iron nanoparticles can avoid being oxidized and maintain their magnetic properties (such as coercivity or blocking temperature) by gold coating. On the other hand, self-assembly of nanoparticles become more and more important because novel collective properties will be produced in the ordered array of nanoparticles (10–12). So in this paper, we will present a detailed study on the synthesis, characterization, and self-assembly of gold-coated iron nanoparticles.

EXPERIMENTAL

All chemicals were purchased from Aldrich and used without further purification. Distilled water was used throughout. All liquid starting materials were degassed for 2 h prior to the experiment. Nanoparticles of Fe@Au were prepared in a reverse micelle of cetyltrimethylammonium bromide (CTAB), using 1-butanol as a cosurfactant and octane as the oil phase. To this mixture, a water solution containing metal ions was added. The size of the reverse micelle is determined by the molar ratio of water to surfactant. Here, a molar ratio of water to CTAB ($\omega = [H_2O]/[CTAB]$) of 8 was selected to prepare the iron nanoparticles. The procedure and components for the experiment are schematically shown in Fig. 1. The iron-containing nanoparticles were separated from those particles that contained just gold using a magnetic field. The final reaction solution was placed in a 0.5 T magnetic field and

[1] To whom correspondence should be addressed. E-mail: jlin@ns.ciac.jl.cn. Fax: + 86-431-5698041.

0022-4596/01 $35.00

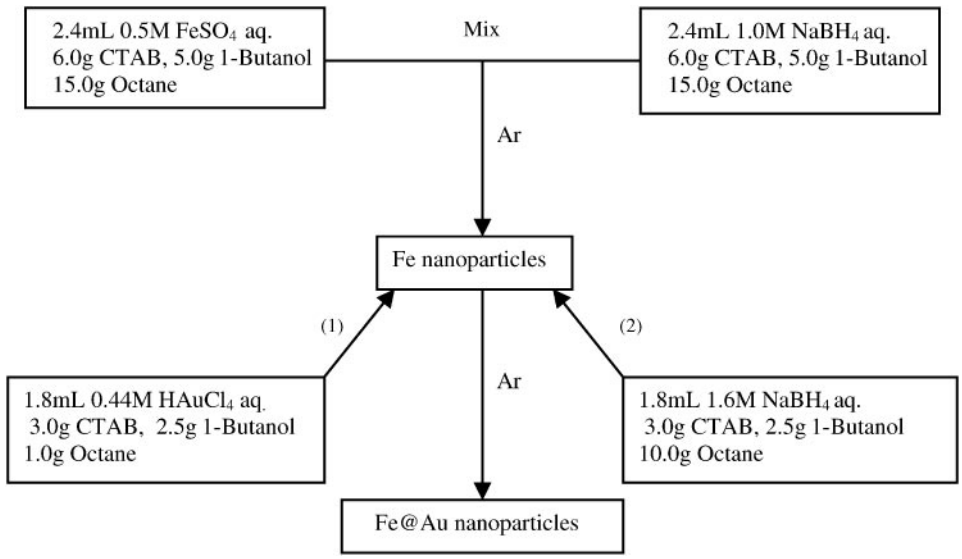

FIG. 1. Schematic diagram showing the procedures of forming Fe@Au nanoparticles.

the Fe@Au nanoparticles were collected using their magnetic properties. The remaining surfactants were removed by thorough washing with a 1:1 chloroform/methanol mixture. The particles were dried under vacuum and stored.

Self-assembly of the Fe@Au nanoparticles was performed by dissolving 10-μg particles in 10 mL of toluene in the presence of 0.2 mL of trioctylphosphine (TOP) and 0.2 mL of 1-dodecanethiol ($C_{12}H_{25}SH$) under ultrasonication. The resulted dispersion was put on a table for several days, producing a precipitate of larger particles and a stable colloid solution of smaller Fe@Au nanoparticles. The latter was dropped on a carbon-coated copper grid under a 0.5 T magnetic field to check its self-assembly situation.

Magnetization measurements were performed on an MPMS-5S SQUID magnetometer. TEM study was carried out on a JEOL 2010 transmission electron microscope. A Phillips X'pert X-ray diffractometer (Cu$K\alpha$ radiation) was used to measure the X-ray diffraction pattern. Light scattering measurements were taken on a DynaPro 99 molecular sizing instrument. UV/vis absorption spectra were recorded on a CARY 500 Scan UV–vis–NIR spectrophotometer.

RESULTS AND DISCUSSION

A. Structural Properties (XRD)

A representative XRD pattern of the Fe@Au nanoparticles is shown in Fig. 2. All the peaks are corresponding to the FCC metallic gold diffraction. The pattern of α-iron is

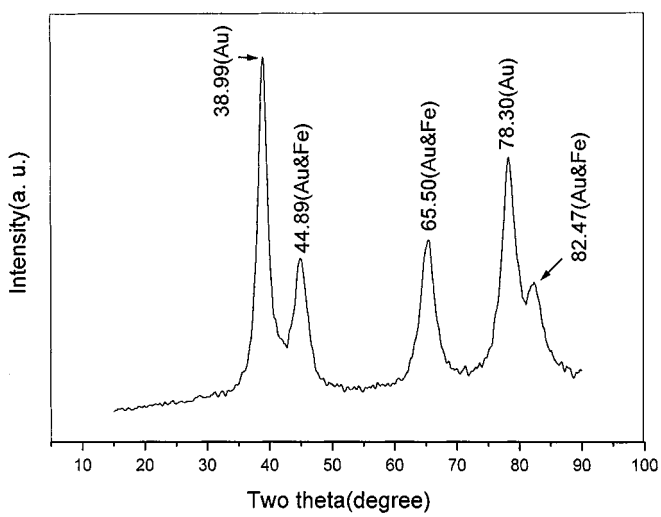

FIG. 2. XRD pattern of the Fe@Au nanoparticles.

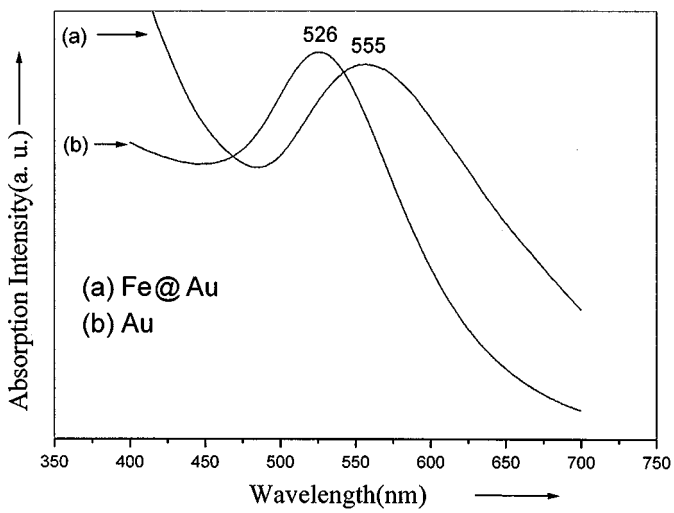

FIG. 3. Absorption spectra of the Fe@Au colloid (a) and Au colloid (b) in toluene.

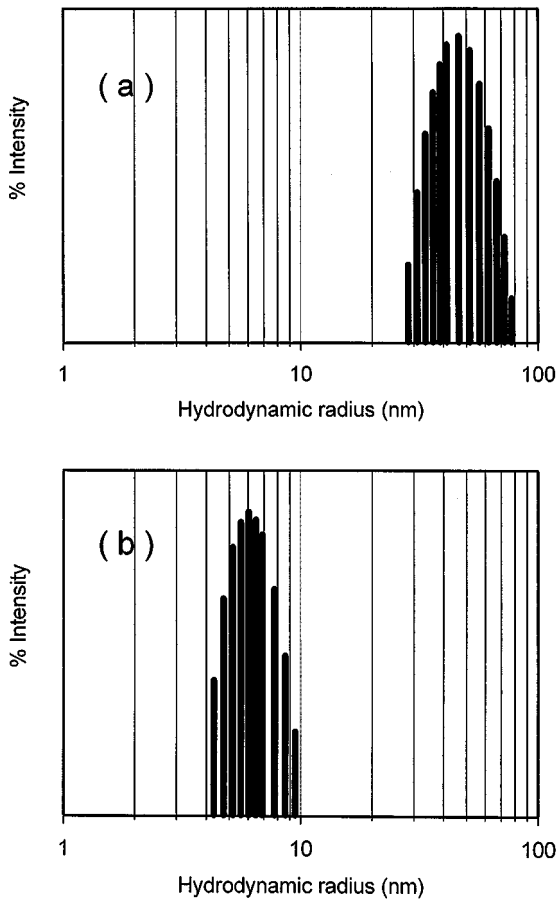

FIG. 4. Histograms of Fe@Au (a) and Au (b) nanoparticles measured by dynamic laser scattering.

hidden under the pattern of gold due to the overlapping of their diffraction peaks at $2\theta = 44.8°$, 65.3°, and 82.5°. Further evidence for the presence of iron in the sample is from an energy-dispersive X-ray spectrum (EDS) attached with a TEM, where the elements sulfur (S), phosphorus (P), copper (Cu), gold (Au), and iron (Fe) have been found. The sulfur and phosphorus are from the added dispertsants (TOP and $C_{12}H_{25}SH$), copper is from the grid, and gold and iron are from the sample. No oxgen is detected in the EDS and no diffraction patterns of iron oxide are observed in the XRD, indicating that the iron nanoparticles are well protected by the gold shell. Other evidence for the structure is from TEM micrographs and magnetic measurements, as discussed later.

B. Optical Properties

The absorption spectrum of the colloid of Fe@Au nanoparticles has been measured, which is compared with that of the pure gold nanoparticle colloid prepared in the same way. The Au colloid shows a red color, while the Fe@Au colloid displays a black-blue color. Figure 3 shows the absorption spectra of the Fe@Au colloid (a) and Au colloid (b). The gold colloid exhibits an absorption band with a maximum at 526 nm, while the Fe@Au colloid shows an absorption band with a maximum at 555 nm. Furthermore, the latter is broader than the former. The absorption of the metallic nanoparticle colloid such as Au, Ag, etc. is due to the surface plasmon absorption (13). The red shift and broadening in the surface plasmon absorption of the Fe@Au colloid relative to the pure Au colloid reveals that the size distribution of pure Au nanoparticles is narrower than that of the Fe@Au nanoparticles and the aggregation of Fe@Au nanoparticles is more serious than the pure Au nanoparticles. This can be confirmed by the results of size distribution measured by laser scattering, as shown in Fig. 4. It is known from Fig. 4 that Au nanoparticles are indeed smaller than Fe@Au nanoparticles, and the former has a narrower size distribution than the latter does. Here, it should be mentioned that light scattering is not able to measure the true size

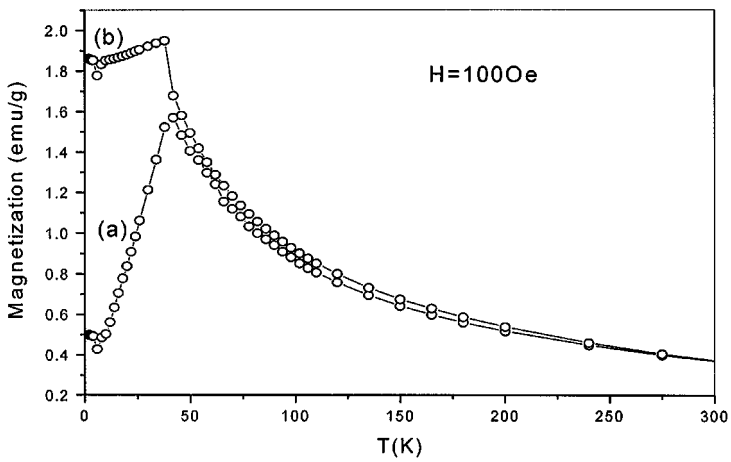

FIG. 5. ZFC/FC curve of Fe@Au nanoparticles: (a) ZFC; (b) FC.

of the particles. The results obtained from light scattering are called hydrodynamic radii, i.e., the size value refers to that of the particles covered by solvent (toluene) and dispersant (TOP, $C_{12}H_{25}SH$) molecules and aggregates of them. Generally, the size obtained from light scattering is much larger than that directly obtained from TEM, which gives the true size of the particles (see Fig. 7, TEM mirograph).

C. Magnetic Properties

Magnetic properties of the dried Fe@Au nanoparticles were derived from zero-field-cooled and field-cooled (ZFC/FC) magnetization as a function of temperature and from magnetization vs magnetic field loops at 2, 10, and 300 K, respectively. The sample was initially cooled in a zero

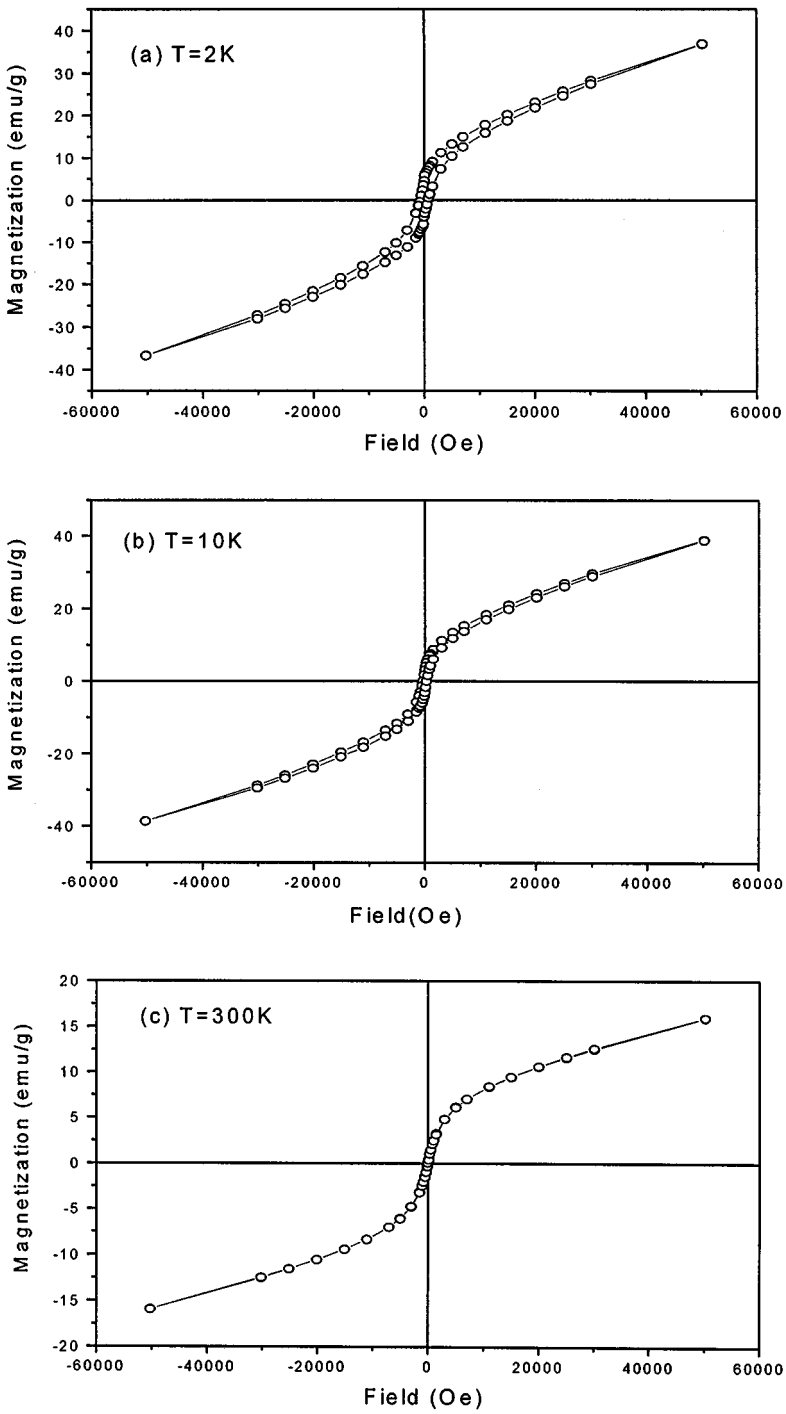

FIG. 6. Magnetization of Fe@Au nanoparticles vs the magnetic field at 2 K (a), 10 K (b), and 300 K (c).

field to 2 K. A 100 Oe field was then applied and magnetization was recorded as the temperature was increased (this is a ZFC curve). When the temperature reached 300 K, the sample was progressively cooled and the magnetization was recorded. This curve is called field-cooled (FC). Figure 5 shows the ZFC/FC curves. In the field-cooled (FC) curve (Fig. 5b), the magnetization nearly stays constant from 2 to 42 K and then shows a uniform decay as the temperature increases. A maximum magnetization can be observed in the ZFC curve (Fig. 5a) at 42 K, indicating that the blocking temperature (T_B) of Fe@Au nanoparticles is 42 K. Below 42 K (T_B), the particles are blocked and in a ferromagnetic state with an irreversible magnetization, whereas above T_B, the magnetization is reversible and the particles are characterized by superparamagnetic behavior (14). The shape of the ZFC curve also suggests a relatively narrower size distribution of the Fe@Au nanoparticles (15).

Figures 6a–6c illustrate the magnetization of Fe@Au nanoparticles as the magnetic field of the susceptometer cycles between $+60$ and -60 kOe at 2, 10, and 300 K, respectively. Below the blocking temperature (42 K), the Fe@Au nanoparticles are in a ferromagnetic state, showing a coercivity and remanence of 728 Oe and 4.12 emu/g at 2 K (Fig. 6a) and 322 Oe and 2.92 emu/g at 10 K (Fig. 6b), respectively. Above the blocking temperature, in the superparamagnetic regime, no coercivity or remanence is observed at 300 K (Fig. 6c). This agrees well with the previous observation (16).

D. Self-assembling Properties

Successful self-assembly of nanoparticle arrays depends on the ability to prepare monodisperse particles and to balance the interparticle forces so that ordered structures form spontaneously. Compared to other self-assembly systems, magnetic nanoparticles have an additional magnetostatic force, which favors the formation of magnetically aligned chains of magnetic dipoles, rather than two- or three-dimensional structures (17).

This is actually the case for our Fe@Au nanoparticles. The self-assembling of Fe@Au nanoparticles was performed under a magnetic field (0.5 T) and checked by TEM. Figure 7 shows the resulted TEM micrographs with different magnifications. In the lower magnification micrograph (Figs 7a), it can be clearly seen that the Fe@Au nanoparticles form some parallel chains with length between 5 and 30μm. Each Fe@Au nanoparticle can be considered as a single domain with a magnetic moment. Under the influence of a foreign magnetic field, these single domains (Fe@Au nanoparticles) aggregate along the direction of a magnetic field and form longer parallel chains. In the higher magnification micrograph (Fig. 7b), a single Fe@Au nanoparticle can be resolved clearly, with a size distribution of 5–15 nm and average size of about 10nm. Furthermore, after careful examination, most of the images of the particles take on a difference in contrast and show core–shell structure.

CONCLUSIONS

The following conclusions can be drawn from this study:

(1) Gold-coated iron nanoparticles (Fe@Au) can be successfully prepared by a reverse micelle approach, which can be characterized by XRD, TEM with EDS, UV/vis absorption spectra, and magnetic measurements.

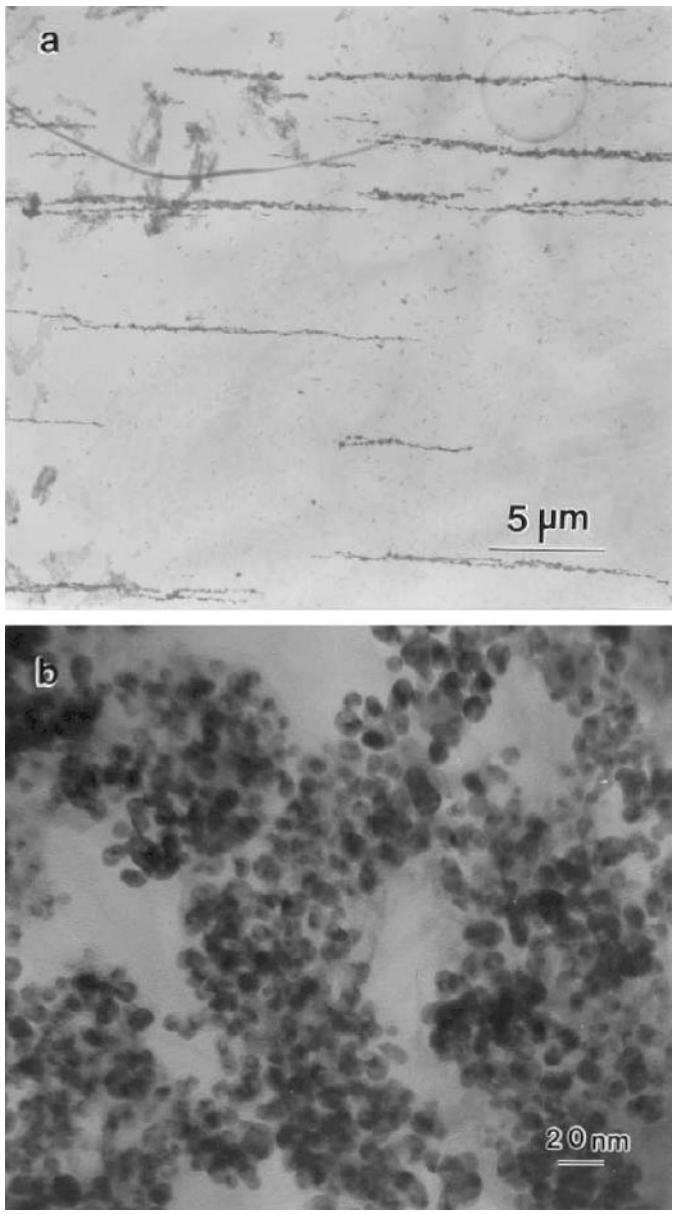

FIG. 7. TEM micrographs of Fe@Au nanoparticles with different magnifications. Dropping of the Fe@Au nanoparticle colloid on the carbon grid was performed under a 0.5 T magnetic field.

(2) The XRD pattern of α-Fe is hidden under the pattern of gold. A red shift and broadening occurs in the absorption band of the Fe@Au colloid compared with that of the pure gold colloid.

(3) The blocking temperature for Fe@Au nanoparticles is 42 K, above which the particles are in a superparamagnetic state and below which in a ferromagnetic state.

(4) These Fe@Au nanoparticles are self-assembled into chains on the micron scale under a magnetic field.

ACKNOWLEDGMENTS

We gratefully acknowledge the support of this work by AMRI through DARPA Grant No. MDA972-97-1-0003 and by Bairen Jihua of Chinese Academy of Sciences.

REFERENCES

1. A. P. Alivisatos, *Science* **271,** 933 (1996).
2. S. Sun, C. B. Murray, D. Weller, L. Folks, and A. Moser, *Science* **287,** 1989 (2000).
3. X. M. Lin, C. M. Sorensen, K. J. Klabunde, and G. C. Hadjipanayis, *Langmuir* **14,** 7140 (1998).
4. F. Bodker, S. Morup, and S. Linderoth, *Phys. Rev. Lett*. **72,** 282 (1994).
5. C. Pathmamnoharan and A. P. Philipse, *J. Colloid Interface Sci.* **205,** 340 (1998).
6. M. Klotz, A. Ayral, C. Guizard, C. Menager, and V. Cabuil, *J. Colloid Interface Sci.* **220,** 357 (1999).
7. D. V. Szabo and D. Vollath, *Adv. Mater*. **11,** 1313 (1999).
8. E. E. Carpenter, C. T. Seip, and C. J. O'Connor, *J. Appl. Phys.* **8,** 5184 (1999).
9. M. Brust, D. Bethell, D. J. Schiffrin, and C. J. Kiely, *Adv. Mater*. **7,** 795 (1995).
10. S. Wirth, S. von Molnar, M. Field, and D. D. Awschalom, *J. Appl. Phys.* **8,** 5249 (1999).
11. S. Sun and C. B. Murray, *J. Appl. Phys.* **8,** 4325 (1999).
12. A. Ngo and M. P. Pileni, *Adv. Mater*. **12,** 276 (2000).
13. A. Taleb, C. Petit, and M. P. Pileni, *Chem. Mater*. **9,** 950 (1997).
14. C. Petit, A. Taleb, and M. P. Pileni, *Adv. Mater*. **10,** 259 (1998).
15. A. S. Waniewska, M. Gutowski, and H. K. Lachowicz, *Phys. Rev. B* **46,** 14594 (1992).
16. E. E. Carpenter, C. Sangergorio, and C. J. O'Connor, *IEEE Trans. Magn.* **35,** 3496 (1999).
17. Y. Jin, C. L. Dennis, and S. A. Majetich, *Nanostrucl. Mater*. **12,** 763 (1999).